Journal of Power Sources 195 (2010) 5801–5805

Contents lists available at ScienceDirect

Journal of Power Sources

journal homepage: www.elsevier.com/locate/jpowsour

Short communication

Influence of gas ambient on the synthesis of co-doped ZnO:(Al,N) films for photoelectrochemical water splitting

Sudhakar Shet [a,b,*], Kwang-Soon Ahn [c], Todd Deutsch [a], Heli Wang [a], Ravindra Nuggehalli [b], Yanfa Yan [a], John Turner [a], Mowafak Al-Jassim [a]

[a] National Renewable Energy Laboratory, Golden, CO 80401, USA
[b] New Jersey Institute of Technology, Newark, NJ 07102, USA
[c] School of Display and Chemical Engineering, Yeungnam University Gyeongsan, 712-749, South Korea

ARTICLE INFO

Article history:
Received 23 February 2010
Received in revised form 16 March 2010
Accepted 16 March 2010
Available online 27 March 2010

Keywords:
ZnO
ZnO:(Al,N)
Co-doping
Gas ambient
Photoelectrochemical
Bandgap

ABSTRACT

Al and N co-doped ZnO thin films, ZnO:(Al,N), are synthesized by radio-frequency magnetron sputtering in mixed Ar and N_2 and mixed O_2 and N_2 gas ambient at 100 °C. The ZnO:(Al,N) films deposited in mixed Ar and N_2 gas ambient did not incorporate N, whereas ZnO:(Al,N) films grown in mixed O_2 and N_2 gas ambient showed enhanced N incorporation and crystallinity as compared to ZnO:N thin films grown in the same gas ambient. As a result, ZnO:(Al,N) films grown in mixed O_2 and N_2 gas ambient showed higher photocurrents than the ZnO:(Al,N) thin films deposited in mixed Ar and N_2 gas ambient. Our results indicate that the gas ambient plays an important role in N incorporation and crystallinity control in Al and N co-doped ZnO thin films.

© 2010 Elsevier B.V. All rights reserved.

1. Introduction

Photoelectrochemical (PEC) water splitting by sunlight for H_2 production is the most renewable approach for using solar energy [1–3]. The PEC properties of numerous metal oxides, *e.g.*, TiO_2, ZnO, Fe_2O_3, and WO_3, have been studied [1,2,4–7]. The photocurrents achieved in ZnO have been modest so far because, like TiO_2, ZnO has a wide bandgap (3.26 eV) that limits its absorption to ultraviolet (UV) light only. Therefore, the bandgap of ZnO must be reduced to shift the absorption into the visible regions to use sunlight more efficiently. Impurity doping in photoactive metal oxides has been known to shift light absorption to longer wavelengths. Both experimental and theoretical studies have reported that nitrogen and carbon doping are effective methods for bandgap narrowing, leading to improved photoresponse in the long-wavelength region [2,8,9]. Similarly, N incorporation into ZnO has been demonstrated to reduce the optical bandgap, leading to absorption in the long-wavelength regions [10,11]. Significant amounts of N can be incorporated into ZnO and WO_3 only at low temperatures [12,13] at which the films grown usually exhibit very poor crystallinity; this is extremely detrimental to the PEC performance. This dilemma hinders the PEC performance of N-incorporated ZnO and WO_3 films. A possible cause for the inferior crystallinity is due to the uncompensated charged N atoms. This problem could be overcome by charge-compensated donor-acceptor doping: for example, co-doping ZnO with Al and N. Furthermore, incorporating (Al,N) pairs is easier than incorporating sole N atoms because of donor–acceptor interaction [14–16]. The Al and N co-doped ZnO films have been synthesized by many groups; however, to date, these studies have focused mostly on p-type doping, and thus, the doping concentration was usually low and the bandgap of ZnO was not heavily affected [17–20]. The effect of passive co-doping of Al and N in ZnO thin films on PEC performance has not been investigated.

In this paper, we report on the synthesis of ZnO:(Al,N) thin films by reactive radio-frequency (RF) magnetron sputtering in mixed Ar and N_2, and mixed O_2 and N_2 ambient. We found that the mixed gas ambient plays a important role in N incorporation in co-doped ZnO:(Al,N) films. Al and N co-doped ZnO in mixed O_2 and N_2 gas ambient, (Al,N)(O_2/N_2), exhibits enhanced N concentration and crystallinity as compared to ZnO:(Al,N)(Ar/N_2), deposited in mixed Ar and N_2, ambient. As a result, ZnO:(Al,N)(O_2/N_2) thin films revealed improved PEC response, compared to ZnO:(Al,N)(Ar/N_2) films. Furthermore, we

* Corresponding author at: National Renewable Energy Laboratory, National Center for Photovoltaic, 1617 Cole Blvd, Golden, CO 80401, USA. Tel.: +1 303 384 7621; fax: +1 303 384 6491.
E-mail addresses: sudhakar.shet@nrel.gov, ss63@njit.edu (S. Shet).

0378-7753/$ – see front matter © 2010 Elsevier B.V. All rights reserved.
doi:10.1016/j.jpowsour.2010.03.058

found that the N concentration in ZnO:(Al,N)(O_2/N_2) thin films can be effectively controlled by co-doping at varying gas flow rate.

2. Experimental

Two sets of ZnO:(Al,N) thin films were deposited by reactive RF magnetron sputtering using a ZnO–2 wt% Al target at 200-W RF power. One set of samples was deposited in mixed Ar and N_2 ambient. We refer to this set of samples as ZnO:(Al,N)(Ar/N_2). The second set of samples was deposited in mixed O_2 and N_2 gas ambient and is referred to as ZnO:(Al,N)(O_2/N_2). F-doped SnO_2 (FTO, 20–23 Ω sq.$^{-1}$)-coated transparent glasses were used as substrates. The distance between the target and substrate was 8 cm. The base pressure was below 5×10^{-6} Torr, and the working pressure for all synthesis was 2×10^{-2} Torr. Prior to sputtering, a pre-sputtering process was performed for 30 min to eliminate any contaminants from the target. Sputtering was then conducted at RF power of 200 W with varying gas flow ratio at a substrate temperature of 100 °C. Substrates were rotated at 30 rpm during deposition to enhance film uniformity. For comparison, ZnO and ZnO:Al films were also deposited in pure Ar ambient using ZnO and ZnO–2 wt% Al targets, respectively. All samples were controlled to have similar film thickness of about 1000 nm as measured by stylus profilometry.

The structure of synthesized films was characterized by X-ray diffraction (XGEN-4000, SCINTAG Inc., operated with a Cu Kα radiation source at 45 kV and 37 mA), and the N concentration in the thin films was evaluated by X-ray photoelectron spectroscopy (XPS). The ultraviolet–visible (UV–Vis) absorption spectra of the samples were measured by an n&k analyzer 1280 (n&k Technology, Inc.) to investigate optical properties.

PEC measurements were performed in a three-electrode cell with a flat quartz-glass window to facilitate illumination to the photoelectrode surface [21,22]. The sputter-deposited films were used as the working electrodes with an active surface area of about 0.25 cm^2. Pt mesh and an Ag/AgCl electrode were used as counter and reference electrodes, respectively. A 0.5-M Na_2SO_4 aqueous solution with a pH of 6.8 was used as the electrolyte for the PEC measurements, and the scan rate was 5 mV s^{-1} in this experiment. The PEC response was measured using a fiber-optic illuminator (150-W tungsten-halogen lamp) with an ultraviolet/infrared (UV/IR) cut-off filter (cut-off wavelengths: 350 and 750 nm) and combined UV/IR and green band-pass filter (wavelength: 538.33 nm, full width at half maximum [FWHM]: 77.478 nm). The light intensity was measured by a photodiode power meter. The total light intensity with the UV/IR filter only was fixed at 125 mW cm^{-2}.

Because our films were deposited on conducting substrates, measurements of electrical property by the Hall Effect were not possible. Instead, the electrical properties were measured by Mott–Schottky plots, which were obtained by alternating current (AC) impedance measurements. AC impedance measurements were carried out with a Solartron 1255 frequency response analyzer using the above three-electrode cells. An AC amplitude of 10 mV and frequency of 5000 Hz were used for measurements taken under dark conditions, and the AC impedances were measured in the potential range of −0.7 to 1.25 V (vs. Ag/AgCl reference). The series capacitor-resistor circuit model was used for Mott–Schottky plots [23,24].

3. Results and discussion

Fig. 1 shows the X-ray diffraction curves of ZnO grown in Ar ambient and ZnO:(Al,N)(Ar/N_2) grown in mixed Ar and N_2 gas ambient with N_2 mass flow rate of 25–75%, respectively. Dotted lines in the XRD plots indicate substrate peaks. We see that the ZnO film exhibits poor crystallinity because of the low-temperature sputtering process. The ZnO:(Al,N)(Ar/N_2) films showed better crystallinity than the ZnO film. The mixed N_2 and Ar gas ambient should be the reason for enhanced crystallinity. No significant change in crystallinity is observed by varying the N_2 mass flow rate from 25% to 75%. One would expect that as the N_2 mass flow rate increases, N incorporation in ZnO film should increase. However, no significant change in crystallinity observed in the film, by increasing the N_2 mass flow rate indicates, that no significant amount of N concentration is incorporated in the film. It is known that a high concentration of dopant can deteriorate crystal structure. However, applying the Debye–Scherrer equation to our XRD data, crystallite sizes were 21, 30, 32, and 37 nm for the ZnO, ZnO:(Al,N)(Ar/N_2) films for 25%, 50%, and 75% N_2 mass flow rate, respectively. These indicate that N may not be incorporated in ZnO even when the samples were deposited in mixed Ar and N gas ambient. Indeed, XPS measurements confirmed that no detectable N concentrations were found in these ZnO:(Al,N)(Ar/N_2) films.

Fig. 2 shows the optical absorption coefficients of the ZnO and ZnO:(Al,N)(Ar/N_2) films. The direct electron transition from valence to conduction bands was assumed for the absorption coefficient curves, because ZnO has a direct bandgap [25,11]. The optical bandgaps of the films were determined by extrapolating the linear portion of each curve. The bandgap of the ZnO film is 3.25 eV, which is consistent with the results reported elsewhere [26]. The direct optical bandgaps measured for ZnO:(Al,N)(Ar/N_2) films with N_2 mass flow rate of 25%, 50%, and 75% are about 3.28, 3.32, and 3.35 eV, respectively, which surprisingly are larger than that of ZnO. These bandgap differences can be understood by the crystallinity of the samples. ZnO has the lowest crystallinity, meaning that it has point defects, such as oxygen vacancies. The presence of these defects introduces impurity bands and leads to a reduced bandgap compared to high-purity ZnO. When the N_2 mass flow rate increased from 25% to 50% to 75%, the crystallinity of ZnO:(Al,N)(Ar/N_2) films increased, as indicated by XRD curves; this means decreased defect concentration. Furthermore, no N was incorporated. Thus, the bandgaps of ZnO:(Al,N)(Ar/N_2) films are generally larger than that of the ZnO grown in pure Ar ambient and the bandgap increased as the N_2 mass flow rate increased.

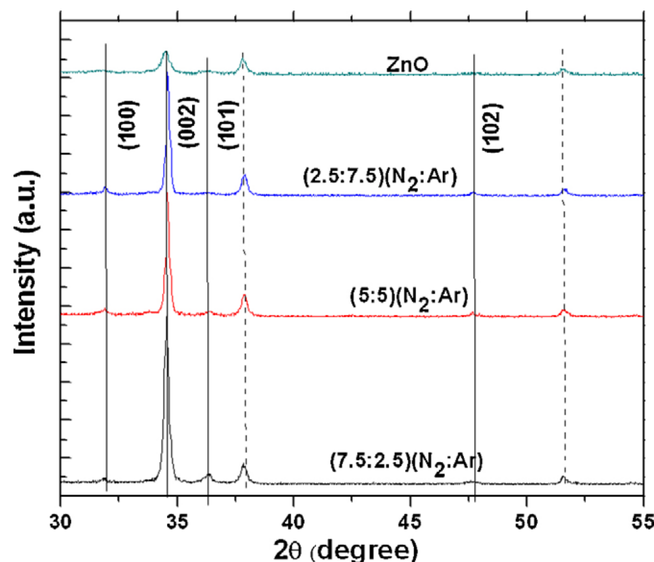

Fig. 1. X-ray diffraction curves of ZnO, and ZnO:(Al,N)(Ar/N_2) films grown at 200 W in Ar and mixed Ar and N_2 gas ambient with N_2 mass flow rate of 25%, 50%, and 75%.

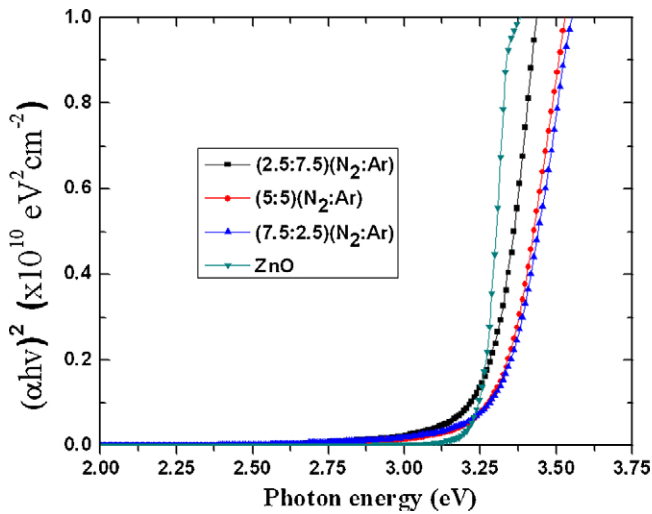

Fig. 2. The optical absorption coefficients of the ZnO and ZnO:(Al,N)(Ar/N_2) films.

Fig. 3(a) shows Mott–Schottky plots of the ZnO and ZnO:(Al,N)(Ar/N_2) films. All the samples exhibited positive slopes, indicating n-type behaviors. It is known from earlier reports that ZnO and Al-doped ZnO films are n-type semiconductors [26,27]. The photocurrent–voltage curves of the ZnO and ZnO:(Al,N)(Ar/N_2) films, under illumination with the UV/IR filter, are shown in Fig. 3(b). It showed clearly that the ZnO:(Al,N)(Ar/N_2) films exhibited enhanced photocurrents, as compared to the ZnO film. The enhanced photocurrent should be due to the increased crystallinity of ZnO:(Al,N)(Ar/N_2) films. At the potential of 1.2 V, the photocurrents were 3.5, 8.5, 14.56, and 18.7 $\mu A\,cm^{-2}$ for the ZnO, ZnO:(Al,N)(Ar/N_2) films with 25%, 50%, and 75% N_2 mass flow rates, respectively. To investigate the photoresponses in the long-wavelength region, a green-color filter (wavelength: 538.33 nm; FWHM: 77.478 nm) was used in combination with the UV/IR filter. The ZnO and ZnO:(Al,N)(Ar/N_2) films exhibited no clear photoresponse, as shown in Fig. 4, confirming that no detectable N was incorporated. The modest photocurrents achieved in ZnO and ZnO:(Al,N)(Ar/N_2) films are because of its wide bandgap, which limits absorption to UV light only. It is clear that the mixed Ar and N_2 gas ambient did not promote N incorporation.

However, when the growth ambient was changed to mixed O_2 and N_2 (second set of samples), N incorporation was observed. Fig. 5 shows the XRD curves of ZnO:Al, grown in Ar ambient and ZnO:(Al,N)(O_2/N_2) films in mixed O_2 and N_2 gas ambient with N_2 mass flow rate of 25%, 50%, and 75%. Dotted lines in the XRD plots indicate substrate peaks. It is seen that the ZnO:Al film exhibits poor crystallinity because of the low-temperature and pure Ar gas ambient. The ZnO:(Al,N)(O_2/N_2) films show better crystallinity than

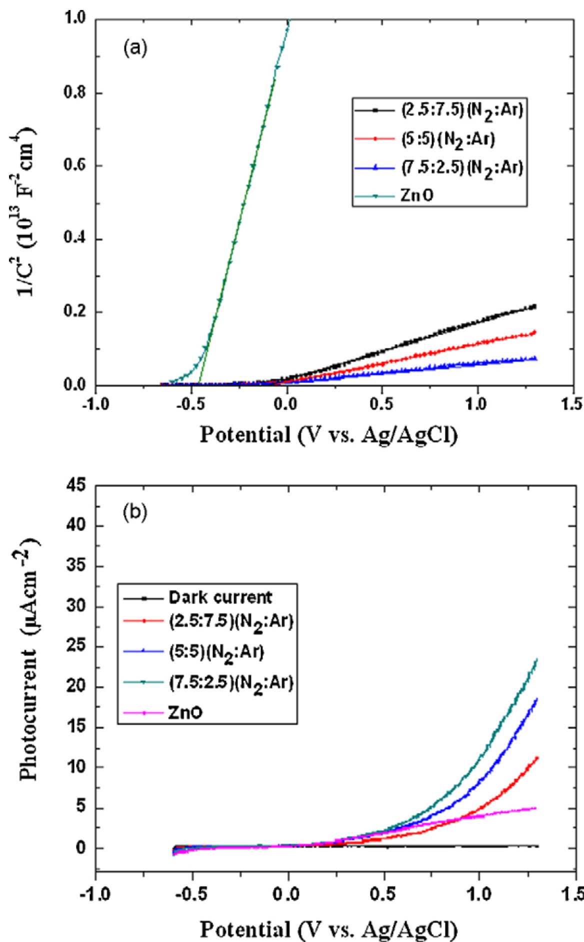

Fig. 3. (a) Mott–Schottky plots of the ZnO and ZnO:(Al,N)(Ar/N_2). (b) Photocurrent–voltage curves of the ZnO and ZnO:(Al,N)(Ar/N_2) films under illumination with the UV/IR filter.

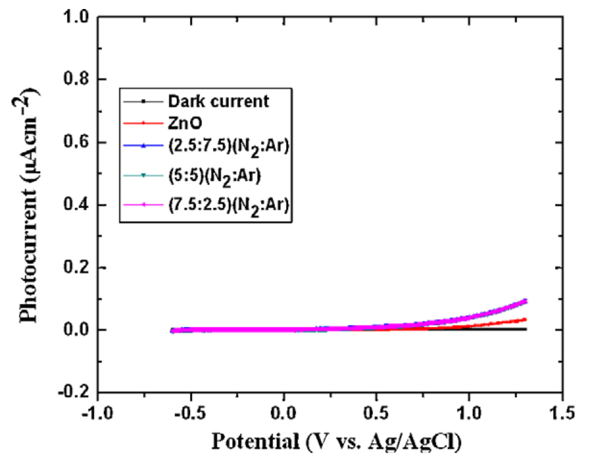

Fig. 4. Photocurrent–voltage curves of the ZnO, ZnO:Al, and ZnO:(Al,N)(Ar/N_2) films under the illumination with the combined green and UV/IR filters.

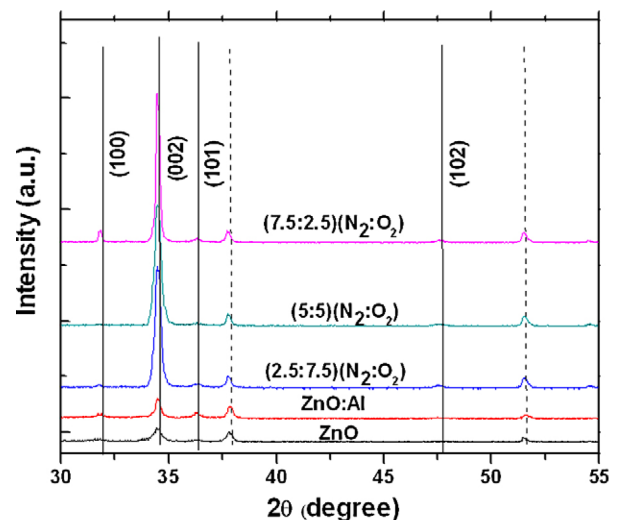

Fig. 5. X-ray diffraction curves of ZnO, ZnO:Al, and ZnO:(Al,N)(O_2/N_2) films grown at 200 W in O_2 and mixed O_2 and N_2 gas ambient with N_2 mass flow rate of 25%, 50%, and 75%.

that of ZnO and ZnO:Al films. The enhancement of crystallinity is attributed to both charge-compensated donor-acceptor co-doping and the mixed O_2 and N_2 gas ambient. We found that the co-doping enhanced the N incorporation in the ZnO:(Al,N)(O_2/N_2) film. The concentrations of N in ZnO:(Al,N)(O_2/N_2) films for 25%, 50%, and 75% N_2 mass flow rate were about 1, 1.6, and 3 at.%, respectively, as determined by XPS. Applying the Debye–Scherrer equation to our XRD data, crystallite sizes were 21, 24, 33, 35, and 40 nm for the ZnO, ZnO:Al, ZnO:(Al,N)(O_2/N_2) films for 25%, 50%, and 75% N_2 mass flow rate, respectively.

Fig. 6(a) shows the optical absorption spectra of the ZnO, ZnO:Al, and ZnO:(Al,N)(O_2/N_2) films. The ZnO and ZnO:Al films showed optical absorption spectra and could absorb light with wavelengths below 450 nm only, due to their wide bandgap. However, the ZnO:(Al,N)(O_2/N_2) films showed optical absorption in the longer-wavelength region, indicating that a significant amount of N has been incorporated into these samples. The optical absorption coefficients of the ZnO, ZnO:Al, and ZnO:(Al,N)(O_2/N_2) films are shown in Fig. 6(b). The bandgap of the ZnO:Al film is 3.35 eV, which is consistent with the results reported elsewhere [27]. The direct optical bandgaps measured for ZnO:(Al,N)(O_2/N_2) films for N_2 mass flow rate from 25% to 75% gradually decreased from 3.13 to 2.85 eV. This reduction in bandgap is due to N-induced upshifting of the valance-band maximum (VBM). It is shown theoretically that the incorporated N would generate an impurity band above the VBM [16]. The absorption from this impurity band cannot be characterized by direct band transitions, and it typically results in an absorption tail in the measured optical absorption curve. Such an absorption tail is clearly evident in Fig. 6(b) for the co-doped ZnO:(Al,N)(O_2/N_2) films. This tail can be considered as further

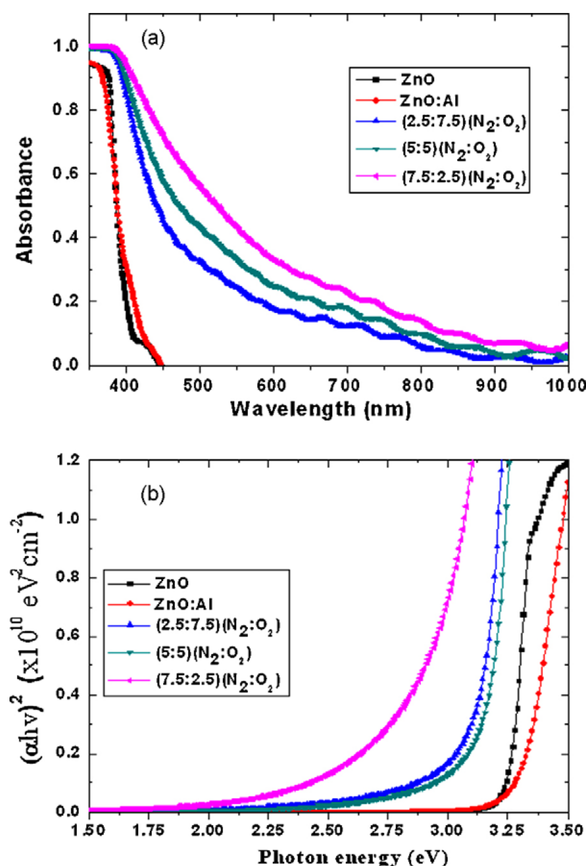

Fig. 6. (a) Optical absorption curves of ZnO, ZnO:Al, and ZnO:(Al,N)(O_2/N_2) films. (b) The optical absorption coefficients of the ZnO, ZnO:Al, and ZnO:(Al,N)(O_2/N_2) films.

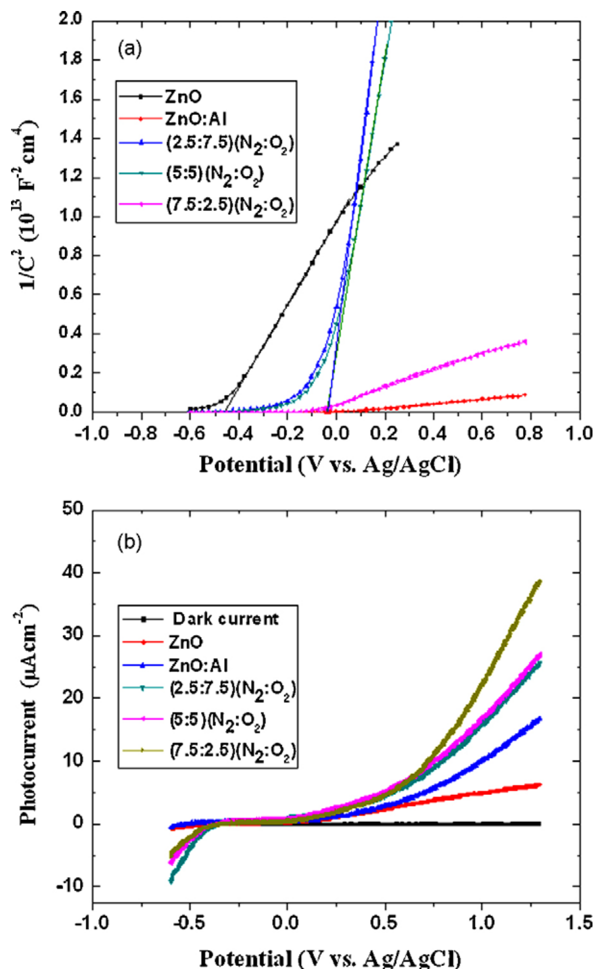

Fig. 7. (a) Mott–Schottky plots of the ZnO, ZnO:Al, and ZnO:(Al,N)(O_2/N_2) films. (b) Photocurrent–voltage curves of the ZnO, ZnO:Al, and ZnO:(Al,N)(O_2/N_2) films under the illumination with the UV/IR filter.

bandgap reduction, which enables light-harvesting in the much longer-wavelength regions as compared to the ZnO, ZnO:Al, and ZnO:(Al,N)(Ar/N_2) films.

Fig. 7(a) shows Mott–Schottky plots of the ZnO:Al and ZnO:(Al,N)(O_2/N_2) films. All the samples exhibited positive slopes, indicating n-type semiconductors. Our previous studies [16,28–31] reported that ZnO:N films deposited under a N_2/O_2 plasma had n-type behavior due to substitutional N_2 molecules that act as shallow double-donors. In ZnO:(Al,N)(O_2/N_2) films, excess Al can also be the source of donors. The photocurrent–voltage curves of the ZnO, ZnO:Al, and ZnO:(Al,N)(O_2/N_2) films, under illumination with the UV/IR filter, are shown in Fig. 7(b). It shows clearly that the ZnO:(Al,N)(O_2/N_2) films exhibited enhanced photocurrents, compared to the ZnO, ZnO:Al, and ZnO:(Al,N)(Ar/N_2) films. The enhanced photocurrent can be attributed to the increased crystallinity, enhanced N incorporation, and compensated charge defects in ZnO:(Al,N)(O_2/N_2) films. At the potential of 1.2 V, the photocurrents were 3.5, 13.24, 21.69, 33.12, and 34.18 $\mu A\,cm^{-2}$ for the ZnO, ZnO:Al, and ZnO:(Al,N)(O_2/N_2) films with 25%, 50%, and 75% N_2 mass flow rate, respectively.

To investigate the photoresponses in the long-wavelength region, a green-color filter was used in combination with the UV/IR filter, as shown in Fig. 8. The ZnO and ZnO:Al films exhibited no clear photoresponse because of their wide bandgap. The co-doped ZnO:(Al,N)(O_2/N_2) films exhibited photocurrents. The results demonstrate clearly that significantly reduced bandgap and enhanced photocurrents can be obtained

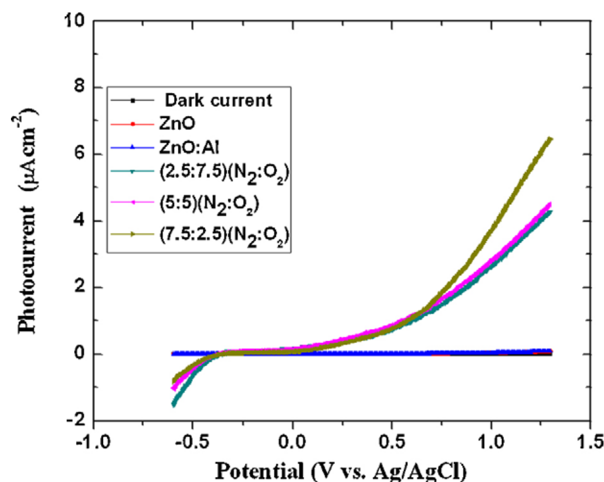

Fig. 8. Photocurrent–voltage curves of the ZnO, ZnO:Al, and ZnO:(Al,N)(O_2/N_2) films under the illumination with the combined green and UV/IR filters.

with mixed O_2 and N_2 gas ambient with varying N_2 mass flow rate and the charge-compensated donor-acceptor co-doping approach.

4. Conclusions

Al and N co-doped ZnO films are synthesized by RF magnetron sputtering in mixed Ar and N_2 and mixed O_2 and N_2 gas ambient at 100 °C. The films deposited under mixed O_2 and N_2 gas ambient showed enhanced N incorporation, whereas ZnO:(Al,N)(Ar/N_2) films grown under mixed Ar and N_2 failed to incorporate any N. The ZnO:(Al,N)(O_2/N_2) films exhibited enhanced crystallinity, yet with successful N incorporation and reduced bandgap. The N concentration is controlled by the gas flow rate of N_2. As a result, Al and N co-doped ZnO films in mixed O_2 and N_2 ambient showed higher photocurrents than that of ZnO films grown in mixed Ar and N_2 ambient. Our results suggest that for effective N incorporation, it is important to select an appropriate gas ambient.

Acknowledgements

This work was supported by the U.S. Department of Energy under Contract # DE-AC36-08GO28308.

References

[1] A. Fujishima, K. Honda, Nature 238 (1972) 37.
[2] R. Asahi, T. Morikawa, T. Ohwaki, K. Aoki, Y. Taga, Science 293 (2001) 269.
[3] O. Khaselev, J.A. Turner, Science 280 (1998) 425.
[4] V.M. Aroutiounian, V.M. Arakelyan, G.E. Shahnazaryan, Solar Energy 78 (2005) 581.
[5] J. Yuan, M. Chen, J. Shi, W. Shangguan, Int. J. Hydrogen Energy 31 (2006) 1326.
[6] G.K. Mor, K. Shankar, M. Paulose, O.K. Varghese, C.A. Grimes, Nano Lett. 5 (2005) 191.
[7] B. O'Regan, M. Grätzel, Nature 353 (1991) 737.
[8] D.N. Tafen, J. Wang, N. Wu, J.P. Lewis, Appl. Phys. Lett. 94 (2009) 093101.
[9] H. Wang, J.P. Lewis, J. Phys. Condens. Matter 18 (2006) 421.
[10] M. Joseph, H. Tabata, T. Kawai, Jpn. J. Appl. Phys. 38 (1999) L1205.
[11] M. Futsuhara, K. Yoshioka, O. Takai, Thin Solid Films 317 (1998) 322.
[12] K.-S. Ahn, Y. Yan, M. Al-Jassim, J. Vac. Sci. Technol. B 25 (2007) L23.
[13] D. Paluselli, B. Marsen, E.L. Miller, R.E. Rocheleau, Electrochem. Solid-State Lett. 8 (2005) G301.
[14] T. Yamamoto, H. Katayama-Yoshida, Jpn. J. Appl. Phys. 38 (1999) L166.
[15] H. Matsui, H. Saeki, H. Tabata, T. Kawai, Jpn. J. Appl. Phys. 42 (2003) 5494.
[16] Y. Yan, S.B. Zhang, S.T. Pantelides, Phys. Rev. Lett. 86 (2001) 5723.
[17] Z.W. Liu, S.W. Yeo, C.K. Ong, J. Mater. Res. 22 (2007) 2668.
[18] J.G. Liu, Z.Z. Ye, F. Zhuge, Y.J. Zeng, B.H. Zhao, L.P. Zhu, Appl. Phys. Lett. 85 (2004) 3134.
[19] G.D. Yuan, Z.Z. Ye, L.P. Zhu, Q. Qian, B.H. Zhao, R.X. Fan, C.L. Perkins, S.B. Zhang, Appl. Phys. Lett. 86 (2005) 202106.
[20] Z.-Z. Ye, F.-Z. Ge, J.-G. Lu, Z.-H. Zhang, L.-P. Zhu, B.-H. Zhao, J.-Y. Huang, J. Cryst. Growth 265 (2004) 127.
[21] S. Shet, K.-S. Ahn, Y. Yan, T. Deutsch, K.M. Chrusrowski, J. Turner, M. Al-Jassim, N.M. Ravindra, J. Appl. Phys. 103 (2008) 073504.
[22] S. Shet, K.-S. Ahn, T. Deutsch, H. Wang, N. Ravindra, Y. Yan, J. Turner, M. Al-Jassim, J. Mater. Res. 25 (2010) 69, doi:10.1557/JMR.2010.0017.
[23] S.-H. Kang, J.-Y. Kim, Y. Kim, H.-S. Kim, Y.-E. Sung, J. Phys. Chem. C 111 (2007) 9614.
[24] J. Akikusa, S.U.M. Khan, Int. J. Hydrogen Energy 27 (2002) 863.
[25] M. Gratzel, Nature 414 (2001) 338.
[26] C.X. Xu, X.W. Sun, X.H. Zhang, L. Ke, S.J. Chua, Nanotechnology 15 (2004) 856.
[27] K.H. Kim, R.A. Wibowo, M. Badrul, Mater. Lett. 60 (2006) 15.
[28] K.-S. Ahn, Y. Yan, S.-H. Lee, T. Deutsch, J. Turner, C.E. Tracy, C. Perkins, M. Al-Jassim, J. Electrochem. Soc. 154 (2007) B956.
[29] C.L. Perkins, S.H. Lee, X. Li, S.E. Asher, T.J. Coutts, J. Appl. Phys. 97 (2005) 034907.
[30] K.-S. Ahn, S. Shet, T. Deutsch, C.-S. Jiang, Y. Yan, M. Al-Jassim, J. Turner, J. Power Sources 176 (2008) 387.
[31] K.-S. Ahn, Y. Yan, S. Shet, T. Deutsch, J. Turner, M. Al-Jassim, Appl. Phys. Lett. 91 (2007) 231909.